Recent Advances in Mechatronics

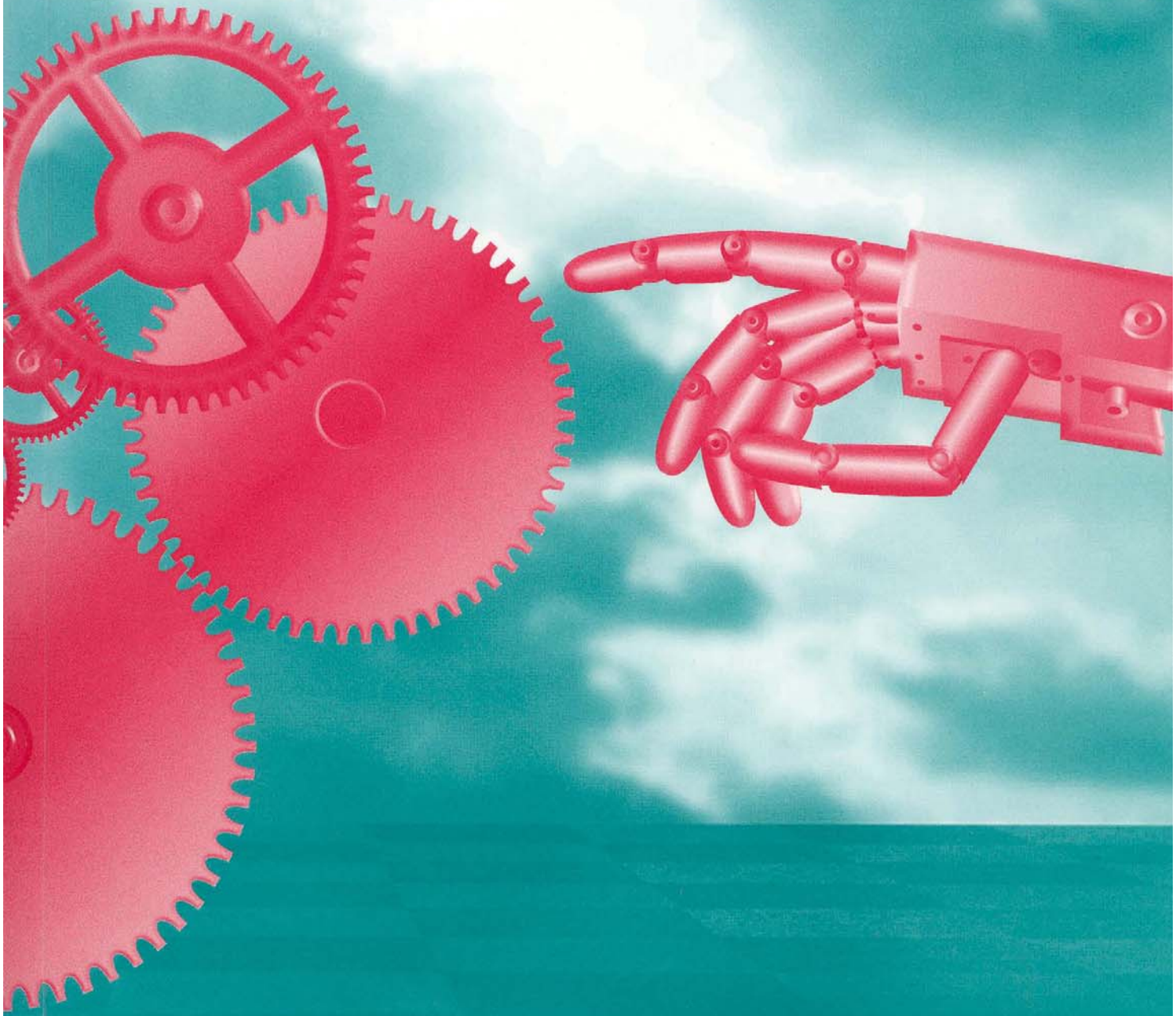

Okyay Kaynak
Sabri Tosunoglu
Marcelo Ang, Jr
(Eds.)

Springer

Performance Issues in Biped Walking Robots

Filipe M. Silva[1] and J.A. Tenreiro Machado[2]

[1] Dept. of Mechanical Engineering
University of Aveiro,
3810 Aveiro, Portugal
fsilva@mec.ua.pt
[2] Dept. of Electrical Engineering
Polytechnic Institute of Porto (ISEP)
Rua de S. Tomé, 4200 Porto, Portugal
jtm@dee.isep.ipp.pt

Abstract. This paper presents the dynamic analysis of robotic biped systems. The main goal is to gain insight into the phenomenon of walking and to evaluate its performance. In this study, we propose three methods to quantitatively measure the dynamic efficiency of walking: energy analysis, perturbation analysis and lowpass frequency analysis. In order to accomplish this goal, the prescribed motion of the biped is completely characterised in terms of a set of locomotion variables, namely: step length, hip height, hip ripple, hip offset, foot clearance and link lengths. Based on these variables and their influence, the performance measures are discussed and the results compared with those observed in nature.

1 Introduction

In the last years a growing field of research in biped locomotion culminated in the development of a large variety of prototypes [1-3]. A retrospective analysis of past legged machines, shows that the design methodologies led to the reproduction of structures, functions and principles found in nature. At the same time, we are still in a primitive stage in understanding the motor control principles and the sensory integration subjacent to human walking. These questions have motivated several researchers in the pursuit of efficient walking robots stimulated by the synergy in the biology and robotic areas. Vukobratovic *et al.* [4] have proposed models and mechanisms to explain biped locomotion. In another perspective, Raibert and his colleagues [5] built hopping and running legged robots in order to study the major issues with dynamic balance.

Bearing this fact in mind, in this article a planar biped is modelled and its performance evaluated according to different viewpoints. The main purposes are threefold:

- To characterise the biped motion in terms of a set of locomotion variables.
- To search for the optimal locomotion variables that minimise the proposed cost functions.
- To establish the correlation among these locomotion variables and the system's performance.

The remainder of the paper is organised as follows. A short description of the biped model is given in section 2. In section 3 we describe the algorithm used to plan the kinematic trajectories of the biped robot. In section 4 various dynamic performance measures are proposed and discussed mathematically. Based on these indices, several numerical results are presented in section 5 to illustrate the application of the proposed methods. Finally, in section 6 we outline the main conclusions and the perspectives towards future research.

2 Biped Model

Figure 1 shows the planar biped model with the notation used throughout this paper. The proposed model consists of seven links in order to approximate locomotion characteristics similar to those of the lower extremities of the human body (*i.e.*, body, thigh, shank). In the present study, we assume that a complete walking cycle is divided in two phases:

- *Single-support phase* - in which one leg is in contact with the ground and the other leg swings forward.
- *Exchange-of-support phase* - in which the legs trade role.

In the single support phase, the stance leg is in contact with the ground and carries the weight of the body, while the swing leg moves forward in preparation for the next step. At the exchange of support, the swing leg contacts the ground with zero velocity to avoid impulsive forces due to the impact phenomenon [6]. The impact of the swing leg is assumed to be perfectly inelastic while ensuring that no slippage occurs. At the same time, the feet maintain a flat contact with the ground.

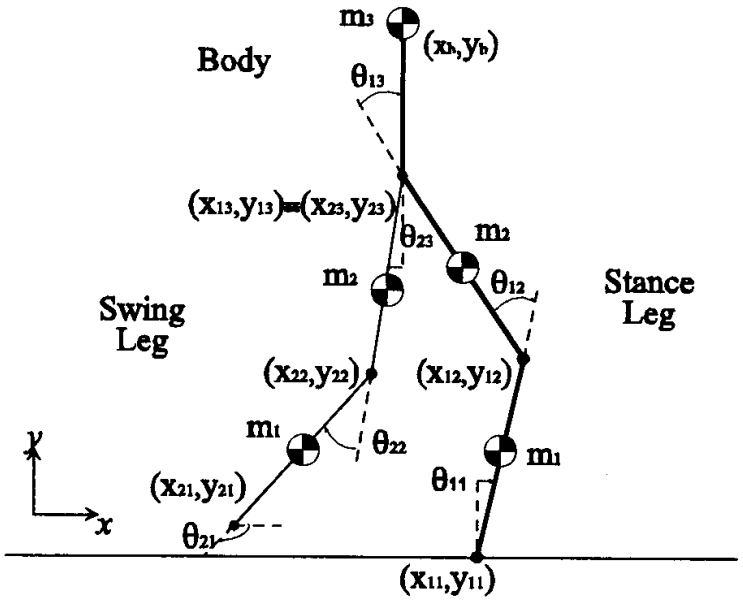

Fig. 1. Planar biped model.

Using the Newton-Euler formulation, we derive the dynamic equations for the seven-link biped that describe the behaviour of a complete single step. The redundancies in the exchange of support are used to satisfy the torque continuity between the single-support and the double-support phases. At the time that the swing leg contacts the ground, an adequate reaction force is prescribed allowing a smooth transition of support. In this study, the ratio of the duration period of exchange of support and complete step is constant (10%).

3 Motion Planning and Evaluation

In early studies, the determination of the biped trajectories was made largely on the basis of experience (*e.g.*, recording kinematic data from human locomotion [9,10]). In this work, the motion planning is accomplished by prescribing the cartesian trajectories of the body and the lower extremities of the leg.

3.1 Locomotion Variables

The motion of the biped system is characterised in terms of a set of variables. The step length L_S is the distance travelled by the body in each step. The hip height H_H is defined as the mean height of the hip along the walking cycle. The hip ripple H_R is measured as the peak-to-peak oscillation magnitude at the hip. The hip offset H_O measures the position of the hip in relation to the middle point between two consecutive contacts of the feet on the ground (*i.e.*, $H_O = D_1 - D_2$).

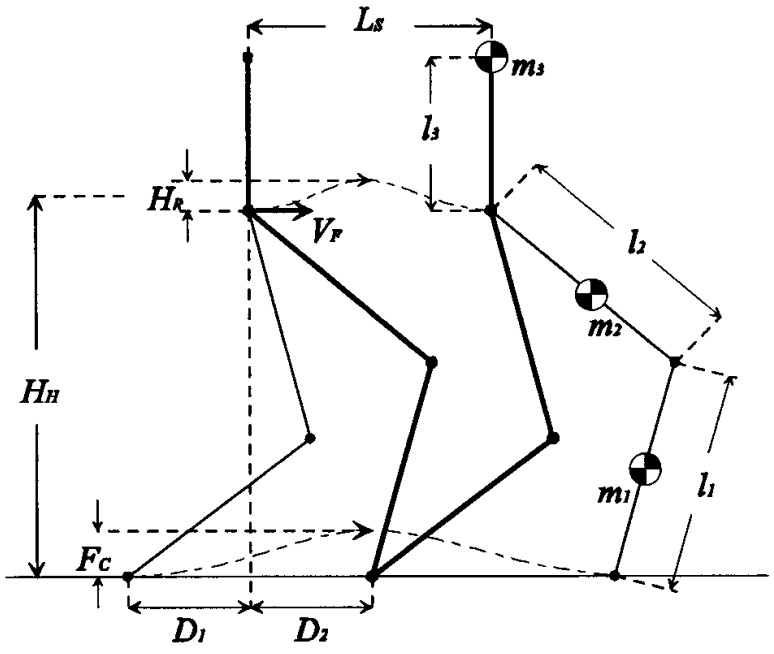

Fig. 2. Locomotion variables.

The foot clearance F_C represents the maximum elevation of the swing foot above the ground. Finally, we examine the role of the link lengths considering that $l_1 + l_2$ assumes a constant value equal to 1 meter (Fig. 2).

3.2 The Trajectory Generator

The proposed algorithm accepts the hip and feet's *Cartesian* trajectories as inputs and, by means of the inverse kinematics, generates the corresponding joint evolution. To improve the smoothness of the motion we impose two restrictions: the body maintains an erect posture and the body forward velocity V_F is constant.

In dynamic walking, at each footfall, the system may suffer impacts and incurs on additional accelerations that influence the forward velocity. For this reason, we impose a set of conditions on the leg velocities so that the feet are placed on the ground while avoiding the impacts. We denote the moment of exchange of support as time t_1, and by t_1^- and t_1^+ the instants just before and after the impact occurs, respectively. For a smooth exchange-of-support, we require that the angular velocities, before and after, to be identical, that is:

$$\dot{\theta}_{2i}(t_1^-) = \dot{\theta}_{1i}(t_1^+). \tag{1}$$

The locomotion parameters characterise completely any configuration in which both feet are on the ground. Nevertheless, between two such configurations there is an infinite number of possible trajectories. In order to simplify the problem, we consider that such motions are produced based on sinusoidal functions. The equation of the tip of the swing leg along the x-axis is computed by summing a linear function with a sinusoidal function. This is implemented using the function:

$$x_{21}(t) = 2V_F\left[t - \frac{1}{2\pi f}\sin(2\pi f t)\right]. \tag{2}$$

where f is the step frequency. Moreover, the vertical motion, that allows the foot to be lifted, has the form:

$$y_{21}(t) = \frac{F_C}{2}\left[1 - \cos(2\pi f t)\right]. \tag{3}$$

The trajectory generator synchronises and coordinates the leg behaviour so that the swing limb arrives at the contact point when the upper body is properly centred with respect to the lower limbs. These trajectories are somewhat restrictive when compared with those of humans where we have ballistic-like motions. In this perspective, the sinusoidal trajectories constitute, merely, a first-order approach to more efficient movements.

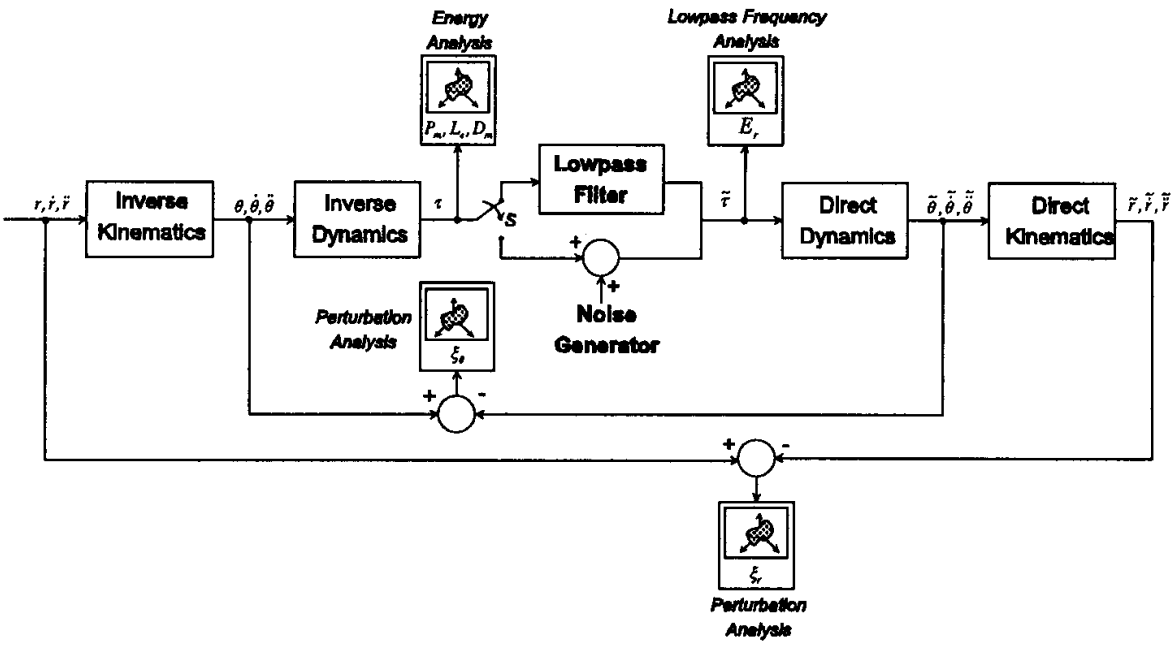

Fig. 3. Block diagram of the performance evaluation.

4 Performance Evaluation

This section covers the implementation of the performance measures used for the dynamic evaluation of the biped system (Fig. 3). In mathematical terms, we shall provide global measures of the overall efficiency in some average sense. The aim is to verify whether a correlation among different view points could be found in walking.

4.1 Energy Analysis

After planning the joint trajectories, we calculate the inverse dynamics in order to map the kinematics into power consumption. The key measure of this analysis is the average mechanical power. It is computed assuming that power regeneration is not available by motors doing negative work, that is, by taking the absolute value of the power. At a given joint j of the leg i, the mechanical power is the product of the motor torque and the angular velocity. The global index is obtained by averaging the mechanical absolute power delivered over a period T:

$$P_m = \frac{1}{T}\sum_{i,j}\int_0^T \left|\tau_{ij}\dot{q}_{ij}\right| dt \ . \tag{4}$$

Although minimizing energy appears to be an important consideration, it may occur an instantaneous near-infinite power demand. In such a case, the average value can be small while the peak is physically unrealizable. As an alternative index, the

standard deviation measure is used to evaluate the dispersion around the mean absolute power:

$$D_m = \sqrt{\frac{1}{T}\int_0^T \left(P_i - P_m\right)^2 dt} \,. \tag{5}$$

where P_i is the total instantaneous mechanical power. For an actuated system, it should be also necessary to consider the average energy lost in the electric motors. This index can be defined as:

$$L_e = \frac{1}{T}\int_0^T \tau^T \tau dt \,. \tag{6}$$

4.2 Perturbation Analysis

In many practical cases the robotic system is noisy, that is, has internal random disturbing forces. As such, an approach called *perturbation analysis* was implemented to determine how the biped model adapts to these distortions. The torque vectors are *'corrupted'* by additive noise using an uniform distribution with zero mean. As result, the trajectories of the system suffer some distortion and can only approximate the desired ones. By computing the forward dynamics and kinematics, we can determine two scalar indices based on the statistical average of the well-known mean-square error (Fig. 3). We can express the indices in terms of the following equations:

$$\xi_\theta = \frac{1}{N_S}\sum_{i=1}^{N_S}\sqrt{\frac{1}{T}\int_0^T \left[\theta_i^r(t) - \theta_i^d(t)\right]^2 dt} \,. \tag{7}$$

$$\xi_r = \frac{1}{N_S}\sum_{i=1}^{N_S}\sqrt{\frac{1}{T}\int_0^T \left[r_i^r(t) - r_i^d(t)\right]^2 dt} \,. \tag{8}$$

where N_S is the total number of steps for averaging purposes, θ_i^r and θ_i^d (r_i^r and r_i^d) are the ith samples of the real and desired angular (linear) displacements. The perturbation analysis is a 'second order' method that measures the system's robustness against variations around the desired trajectory. The stochastic perturbation penalizes the system's smoothness and we shall be concerned with minimizing both ξ_θ and ξ_r.

4.3 Lowpass Frequency Analysis

In robotics, the electro-mechanical system that regulates the movement (*e.g.*, actuators and drives) is constrained by its bandwidth. Hence, the practical conditions

of motor control should also be considered when evaluating the system's performance. In this perspective, the torque variables are expanded in Fourier series and the time domain signals are described by the coefficients of its harmonic terms. Afterwards, these series are filtered through the same lowpass filter. In order to determine the degradation occurred we use, as our figure of merit, the ratio between the energy of the filtered signal E_F and the energy of the original signal E_S, that is:

$$E_r = \frac{E_F}{E_S}. \tag{9}$$

This method, based on the frequency domain has also been successfully employed. However, it is a less general method, because it requires the a priori knowledge about the nature of the robotic actuators.

5 Simulation Results

In this section, we describe the simulation results obtained using the different performance indices. At this stage, the relative performance indices by itself are not sufficient to address the issues of dynamic stability or control. The main purpose is to determine the implications of the locomotion variables on the cost functions and to compare the results with biological data. The simulations are carried out considering a total system mass and body height of $M = 70Kg$ and $L = 1.8m$, respectively.

Table 1. The robot link lengths and masses.

i	l_i (m)	m_i (Kg)
1	0.5	4.0
2	0.5	7.5
3	0.3	47

5.1 Step Length and Hip Height

In a first case study we analyse (Fig. 4) the performance index with respect to the step length and the hip height. For convenience, the chart portion corresponding to hip heights lower than 0.5 m is not represented. One trajectory that undergoes smooth motion is the body flat trajectory in which the stance leg adjusts itself so that the hip maintains a constant height. The body of the robot is assumed to be moving horizontally with a constant forward velocity $V_F = 1\,ms^{-1}$. Furthermore, it is considered that the swing foot stays always on the ground. The system performance is particularly sensitive to the body mass above the hip. Therefore, the link length *vs* mass values adopted in this study are based on anthropometric data [7-8] (Table 1).

As shown in Fig. 4-*a*, to minimize the average mechanical power P_m the hip height must be about 90% of the body height, with optimal step lengths in the range of 0.3-0.6 *m*. Moreover, an important degradation occurs for small step lengths. In Fig. 4-*b*, we depict the results when evaluating the energy lost L_e. The performance surface presents a similar evolution, but L_e is minimized for a slightly higher hip height. At the same time, these results agree with those observed in human locomotion when a subject is allowed to walk without the imposition of a pace frequency constraint.

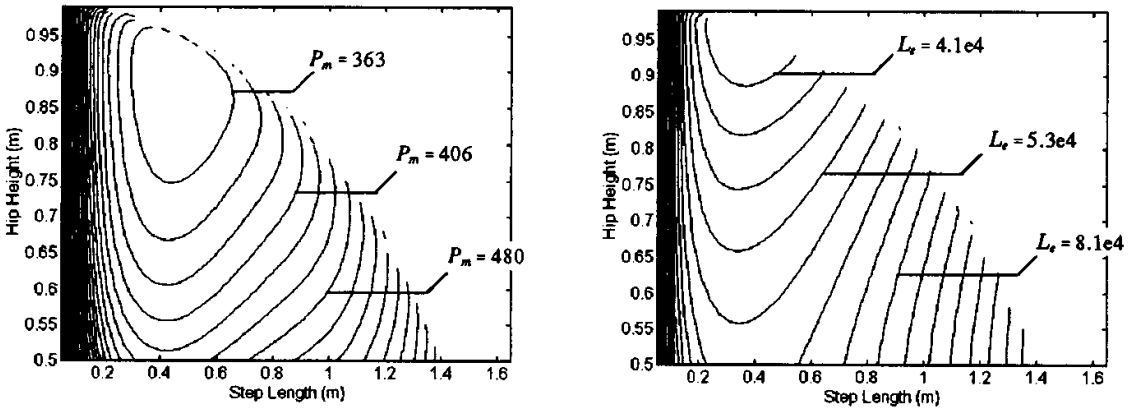

(*a*) (*b*)

Fig. 4. Contour plot: (*a*) mean mechanical power P_m *vs* H_H *and* L_S; (*b*) mean power lost L_e *vs* H_H *and* L_S.

Now, let us examine the "*lowpass frequency analysis*" method. For an ideal lowpass filter whose cutoff frequency is $f_c = 5\,\text{Hz}$, the performance surface E_r is illustrated in Fig. 5-a. At this phase, we calculate also the mean square error of $\tau(t) - \tilde{\tau}(t)$ (see Fig. 5-b).

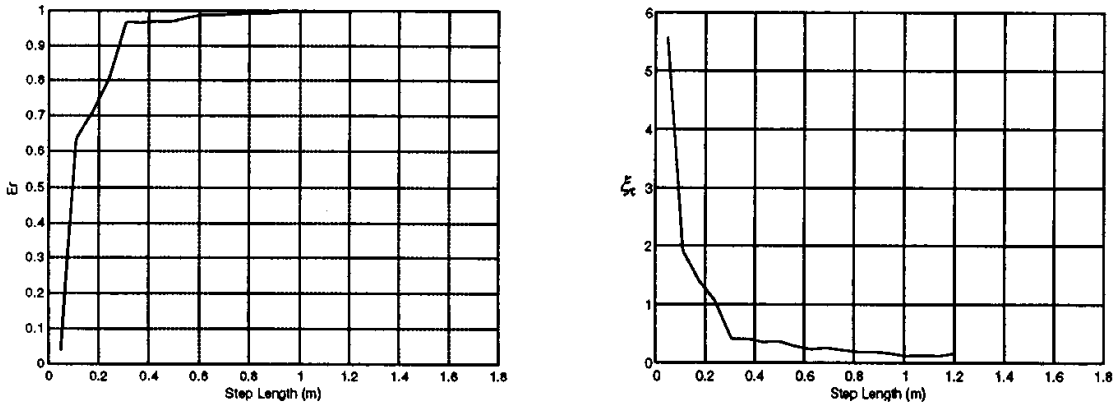

(*a*) (*b*)

Fig. 5. Lowpass frequency analysis: (*a*) energy ratio E_r *vs* L_S; (*b*) mean square error ξ_τ *vs* L_S $\left(H_h = 0.6\,m\right)$.

The discontinuity points solely depend on the number of harmonic terms up to f_c. In contrast to the other methods above, these results suggest that there is an optimum solution for higher step length values, while the performance remains almost unchanged to hip height variations.

5.2 Hip Ripple

In this sub-section, we consider a hip trajectory with a sinusoidal oscillation, while the foot of the swing leg slides over the ground surface. The contour plot in Fig. 6-a suggests that a small adjustable oscillation at the hip may be advantageous in terms of mechanical power. At the same time, the optimum value remains almost unchanged to hip height variations.

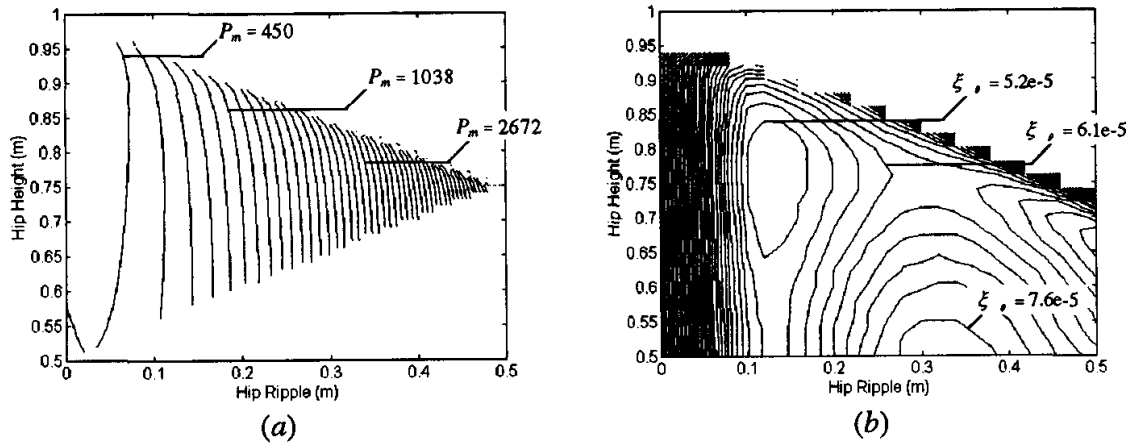

Fig. 6. Contour plot: (*a*) mean mechanical power P_m *vs* H_H *and* H_R ; (*b*) mean perturbation ξ_θ *vs* H_H *and* H_R $\left(L_S = 0.4\ m \text{ and } H_O = F_C = 0\ m\right)$.

A similar phenomenon can be observed in biological systems as well as in previous studies concerning the kinematic analysis of biped locomotion systems [9]. At the same time, the results obtained with the perturbation index ξ_θ (see Fig. 6-b) indicate the advantage in applying ripple to increase the system's robustness against noise.

5.3 Hip Offset

The desired leg coordination is established by assuring that the swing leg arrives at the contact point when the upper body is properly centred with respect to both feet. However, the experiments carried out indicate the advantage of applying a small offset to the hip. Fig. 7 represents the contour plot of two cost functions in terms of hip offset and hip height.

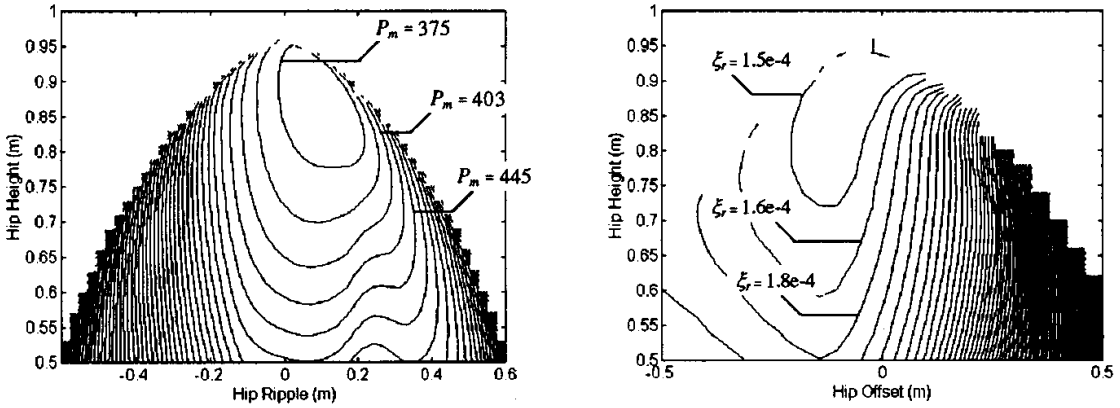

(*a*) (*b*)

Fig. 7. Contour plot: (*a*) mean mechanical power P_m *vs* H_H *and* H_O ; (*b*) mean perturbation ξ_r *vs* H_H *and* H_O $\left(L_S = 0.4\ m \text{ and } H_R = F_C = 0\ m\right)$.

Considering the above plots, two features can be pointed out:

- The optimal hip offset from the viewpoint of energy (perturbation) is a small positive (negative) value.
- The optimal hip offset tends to zero as the hip height increases for both indices P_m and ξ_r.

From this simulation, we can observe an opposite behaviour suggesting a compromise in the final result. The benefits of a small hip offset results from the fact that, during walking, the legs move back and forth to provide, simultaneously, propel and balance actions.

5.4 Foot Clearance

Until now, all the experiences considered that the foot stays on the ground without any friction. Next, we analyse the situation in which the foot can be lifted off the ground. Fig. 8-a shows the influence of the foot clearance variable when using the absolute power and the perturbation analysis. In terms of the index P_m, the minimum foot clearance (except when avoiding any accidental contact) is the optimal one. Although less efficient from the P_m perspective, we believe that the foot clearance is responsible for the system's robustness in uneven walking surfaces. We can observe this process in one-year-old infant's first steps knowing that walking will be learned.

The results obtained with the perturbation index ξ_θ are shown in Fig. 8-b. It was confirmed that a zero foot clearance optimise the system's performance, except for a narrow range of higher hip heights. This means that such cost functions may not be appropriated in this circumstances.

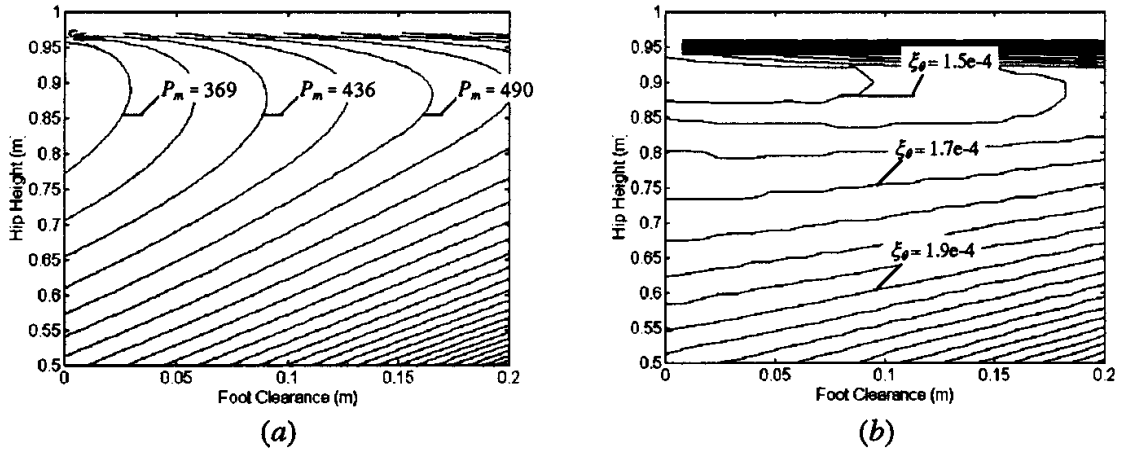

(*a*) (*b*)

Fig. 8. Contour plot: (*a*) mean mechanical power P_m *vs* H_H and F_C; (*b*) mean perturbation ξ_θ *vs* H_H and F_C $\left(L_S = 0.4\ m \text{ and } H_R = H_O = 0\ m\right)$.

5.5 Relative link lengths

This sub-section investigates the role of the relative link lengths in the system's performance considering $l_1 + l_2 = 1m$. The minimum mechanical power P_m occurs for link lengths $l_1 = 0.65$ and $l_2 = 0.35m$. The values of mean power are plotted against link length l_1 in Fig. 9-a. Moreover, the results indicate that for l_1 in the range from 0.4 to 0.8 m the performance index remains almost constant. On the other hand, the point of minimum ξ_θ corresponds to a slightly smaller knee-ankle length, whilst the curve values change considerably around the minimum (Fig. 9-b).

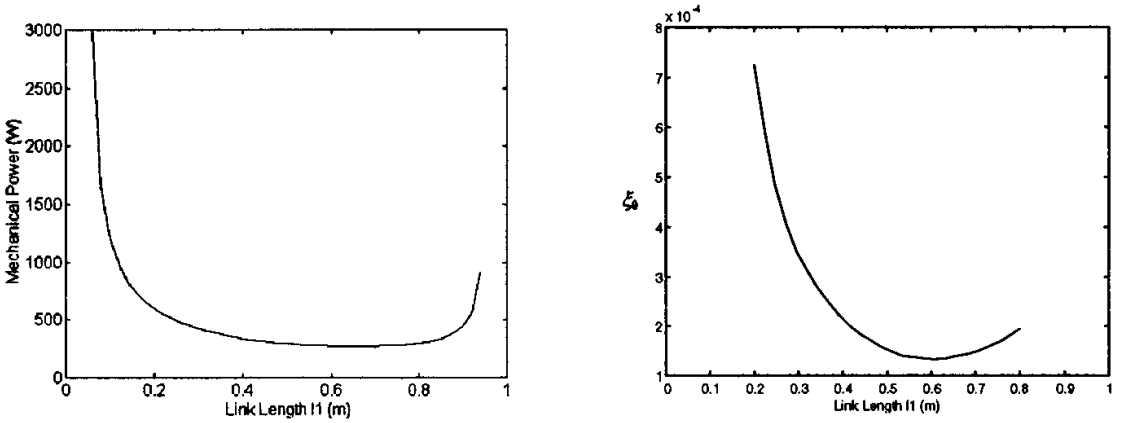

(*a*) (*b*)

Fig. 9. Performance index: (*a*) mean mechanical power P_m *vs* link length l_1; (*b*) mean perturbation ξ_θ *vs* link length l_1.

6 Conclusions

In this paper, we have studied several aspects of biped locomotion. By implementing different motion patterns, we estimated how the robot reacts to a variety of locomotion variables: step length, hip height, hip ripple, hip offset, foot clearance and link lengths. The performance indices used provide a way to evaluate the system's behaviour during normal walking. Moreover, the simulation results could be used to gain insight into the implications of many design and motion planning parameters on the energy efficiency of a bipedal system.
Future work will address the refinement of our models to include other phenomena of the gait, such as lateral balance and zero ankle torque. At an higher level, it is essential to explore complementary performance measures (*e.g.*, stability, obstacle avoidance) for the generation of efficient motion strategies.

Acknowledgments

The first author is supported by the Fundação para a Ciência e a Tecnologia under grant PRAXIS XXI/BD/9541/96.

References

1. J-I Yamaguchi, A. Takanishi and I. Kato, "Development of a Biped Walking Robot Adapting to a Horizontally Uneven Surface", *Proc. Int. Conf. on Intelligent Robots and Systems*, pp. 1156-1163, 1994.
2. S. Kajita, K. Tani, "Experimental Study of Biped Dynamic Walking", *IEEE Control Systems*, pp. 13-19, 1996.
3. K. Hirai, M. Hirose, Y. Haikawa and T. Takenaka, "The Development of Honda Humanoid Robot", *Proc. IEEE Int. Conf. on Robotics and Automation*, pp. 1321-1326, Leuven, Belgium, 1998.
4. M. Vukobratovic, B. Botovac, D. Surla and D. Stokic, *Biped Locomotion: Dynamics, Stability, Control and Applications*, Springer-Verlag, 1990.
5. M.H. Raibert, *Legged Robots that Balance,* The MIT Press, 1986.
6. Y.F. Zheng and H. Hemami, "Impact Effects of Biped Contact with the Environment", *IEEE Trans. Syst. Man Cyber.*, Vol. 14, n. 3, pp. 437-443, 1984.
7. D.A. Winter., *Biomechanics and Motor Control of Human Movement*, John Wiley & Sons, 1990.
8. J. Basmajian and C. Luca, *Muscles Alive: Their Functions Revealed by Electromyography*, Williams & Wilkins,1978.
9. F. Silva and J.A. Tenreiro Machado, "Kinematic Aspects of Robotic Biped Locomotion Systems", *Proc. IEEE Int. Conf. on Intelligent Robots and Systems*, IROS'97, Vol. 1, pp. 266-271, 8-13 Sept., Grenoble, France, 1997.
10. F. Silva and J.A. Tenreiro Machado, "Towards Efficient Biped Robots", *Proc. IEEE Int. Conf. on Intelligent Robots and Systems*, IROS'98, 13-17 Oct., Victoria, Canada, 1998.